NUMERICAL ORBIT TRACKING IN 3D THROUGH THE INJECTOR CYCLOTRON FOR HEAVY IONS AT iTHEMBA LABS

J. G. de Villiers*, J. I. Broodryk, J. L. Conradie, F. Nemulodi, R. W. Thomae,
iThemba LABS, Somerset West, South Africa
J. J. Yang, T. J. Zhang, CIAE, Beijing, China

Abstract

The electric and magnetic fields of the second injector cyclotron (SPC2) [1] were modelled in 3D with finite element methods, using OPERA-3d [2], in an effort to determine the cause of the relative poor 5% beam transmission through the machine in the 8-turn mode. Simulation of the particle motion was done using machine operational parameters for acceleration of a $^{20}Ne^{3+}$ beam.

Using TOSCA [2], an isochronous magnetic field was calculated from a complete cyclotron magnet model and the electrostatic field distribution from a dee electrode model. The SOPRANO-EV [2] modelling of the RF resonance conditions of the resonators provided radial electric field profiles in the acceleration gaps.

A command line program was developed to combine the information of the three models and implement time-dependent control of the electrostatic fields during the particle tracking.

In addition, based on calculated data from OPERA-3D, the parallel particle-in-cell code OPAL-CYCL [3, 4] was used to calculate a particle orbit for comparison.

SIMULATION MODELS AND CONTROL

General

The SPC2 pre-accelerates heavy ion beams before injection into the separated sector cyclotron. The beam from one of the two external ion sources is axially injected upwards and bent into the median plane of SPC2 through a spiral inflector. It is a solid pole cyclotron with 4 radial magnet sectors and 8 trim coils. The electric fields in the 4 acceleration gaps are provided by two horizontal λ/4 coaxial resonators with 90° dees that operate in the frequency range 8.6 MHz to 26 MHz [5].

Simulating the 8-turn orbit mode in SPC2 requires cyclotron settings such that a particle crosses 34 acceleration gaps before reaching the electrostatic extraction channel (EEC), followed by another acceleration gap crossing before exiting the machine. The horizontal width of the EEC gap at the entrance is 14 mm and its radial centre position is adjustable between 456 and 470 mm.

The calculations reported here are based on known operational conditions for a $^{20}Ne^{3+}$ beam with an extraction energy of 3.81 MeV, for acceleration at a harmonic number of 6 and peak dee voltage of 37.4 kV at 12.16 MHz. The spiral inflector voltage and ion source extraction voltages are 4.3 kV and 13.37 kV, respectively.

The magnetic flux density in the centre is 0.88 T.

---

*gdevil@tlabs.ac.za

Cyclotron Magnet Model

The finite element model of the SPC2 magnet includes all geometrical detail of the steel and coils, together with the axial hole in the yoke that, amongst others, contains solenoids and steerer magnets in the lower half of the yoke. The known magnetic material characteristics of the iron are used in the simulation.

The same magnet model was used to build a database that is used to predict the coil currents required for isochronous magnetic fields at different particle energies [6].

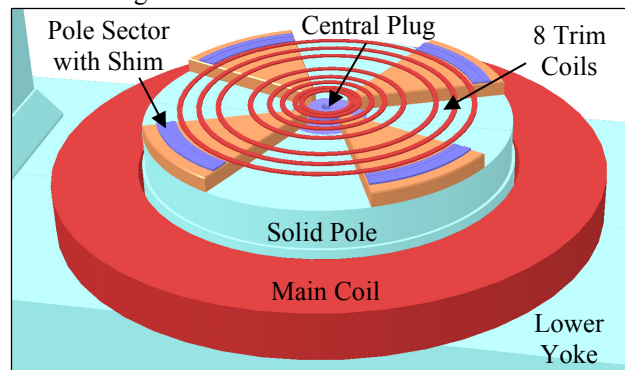The lower pole geometry of the magnet and coils are shown in Fig. 1.

Figure 1: The lower half of the magnet pole geometry, including 4 pole sectors, shims and coils.

Acceleration Electrode Model

In order to obtain the fields in the acceleration gaps under RF conditions, the electric field profile in each acceleration gap was calculated with a model for each of the two RF resonators, using the eigenvalue solver of SOPRANO. The model shown in Fig. 2 includes the dees, dummy dees, puller, capacitors, short-circuit plates and central region, but without the inflector. The calculated normalized field values are shown in Fig. 3.
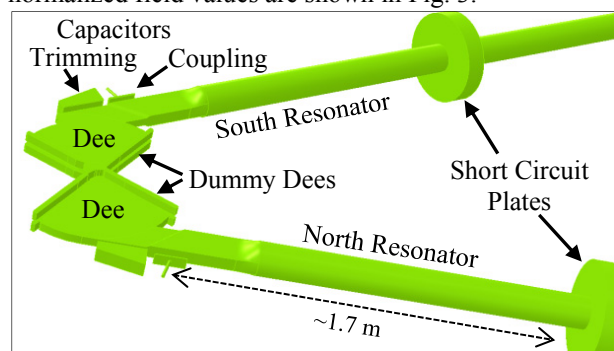

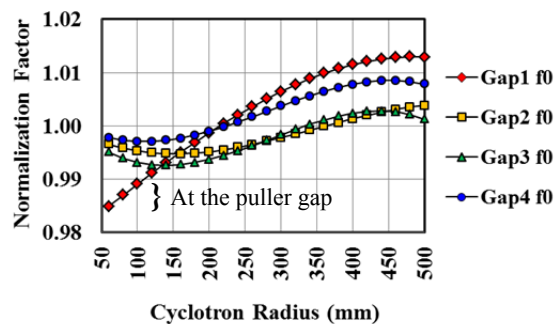Figure 2: Model of the RF resonators without the outer conductors.

Figure 3: The calculated radial field profiles. (See Fig. 5 for the gap numbering).

Another model of the electrodes, which includes the inflector, was used to calculate the static electric field distribution with TOSCA. During particle tracking, the calculated normalized values of the RF fields are used to adjust the static electric field distribution.

The calculated effective lengths of the puller gap and subsequent 3 acceleration gaps are, respectively, 2.5 and 3.2 times larger than the respective physical lengths of 7.3 and 10 mm.

Control Program

An OPERA-3d command line program is used to combine the calculated data of the simulation models and define parameters for adjusting the conditions during the tracking of the particles through the cyclotron. The conversion of the calculated static electric field, E_s, to a time- and positional dependent field, is given by $E_t = A_R.E_s.sin(2\pi f t + \phi_0)$, where f is the RF frequency, ϕ_0 the injection phase of the particle to the dee voltage and t the time-of-flight parameter [7] that is inherently available when particle tracking is done in OPERA-3d POST [2]. The radial adjustment parameter of the RF field amplitude in an acceleration gap, A_R, is calculated in-flight from the applicable radial function shown in Fig. 3. Minor adjustments in the control program permit calculations at other harmonic numbers, implementation of alternative optimization methods and, if needed, to have flat-topping included.

RESULTS OF CALCULATIONS

A single reference particle orbit was calculated, which starts from the vertical injection axis in the centre of the cyclotron. The injection energy and inflector voltage were adjusted to deliver the particle onto the median plane after the inflector. The radial position of the particle at the entrance to the EEC and the extraction energy were optimized by adjusting its injection phase and the dee voltage, using the calculated magnetic field.

Starting on the median plane from a point between the inflector and puller, the central particle orbit was also calculated with OPAL-CYCL. Identical input parameters were used, but the radial correction factor on the dee voltage, A_R, was not implemented for OPAL-CYCL. The positions of the orbits agree well, as shown in Fig. 4.
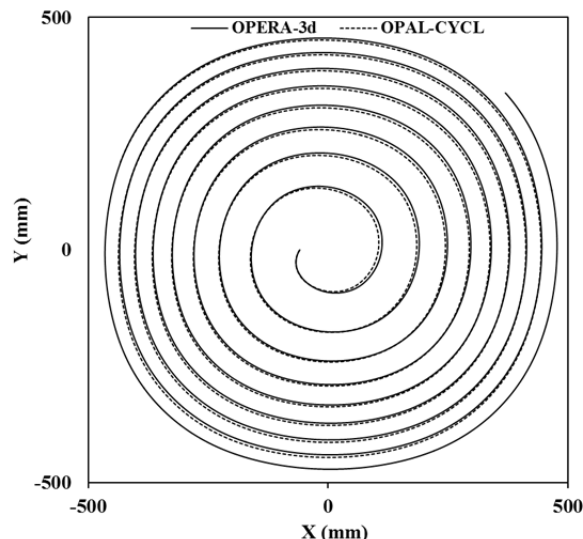

Figure 4: A comparison of the calculated orbits of the reference particle at harmonic number 6 with OPERA-3d (solid line) and OPAL-CYCL (dashed line) shows very good agreement.

A longitudinal bunch length of 14 RF degrees was simulated by using two more particles, one leading and the other lagging by 7 RF degrees from the injection phase of the central reference particle. The injection phase and dee voltage were adjusted to minimize energy spread at extraction, further referred to as optimization method 1 (OM1). The three particles were tracked from a starting position after the inflector and optimized to pass through the EEC with a radial beam width of 5 mm and energy spread of 1.3% at an extraction energy of 4.01 MeV.

For multi-particle tracking horizontal and vertical phase ellipses of 10 π mm.mrad were tracked through the machine for each of the three reference particles that define the longitudinal bunch length of 14 RF degrees.

Using OM1, the energy spread in the beam after one turn is a high 30.7% at beam energy 0.417 MeV, which implies that beam losses for high intensity beams should be expected up to extraction. The transit-time factors are 0.932 and 0.868 for the puller gap and subsequent gaps, respectively. At extraction the energy spread is 2.99% at 4.02 MeV. The calculated orbits are shown in Fig. 5.

The same beam was tracked by using another beam optimization method (OM2). It comprises an iterative process of improving the beam centring, field isochronization and injection phase corrections, and finally by changing of the injection angles of the leading and lagging particles in the beam bunch, respectively, by +1° and -1° from that of the central particles. The last step of differentiated injection angles cannot be implemented in SPC2 at this stage. The energy spread after one turn is 6% at beam energy 0.401 MeV and 1.5% at extraction energy 4.04 MeV. The optimized orbits are shown in Fig. 6. The calculated phase history of the central particle, with the 9 crossings of the centre of the first acceleration gap, is shown in Fig. 7.
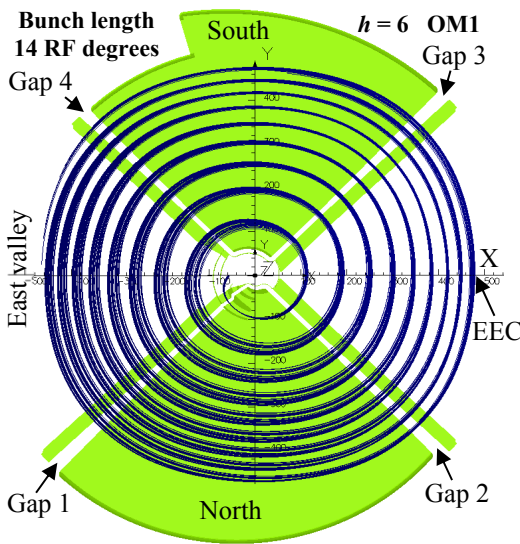
Figure 5: The calculated beam orbits for initial horizontal and vertical beam emittance of 10 π mm.mrad and a longitudinal bunch length of 14 RF degrees, optimized with OM1. The orbits are shown superimposed on the lower half of the model of the acceleration electrodes.
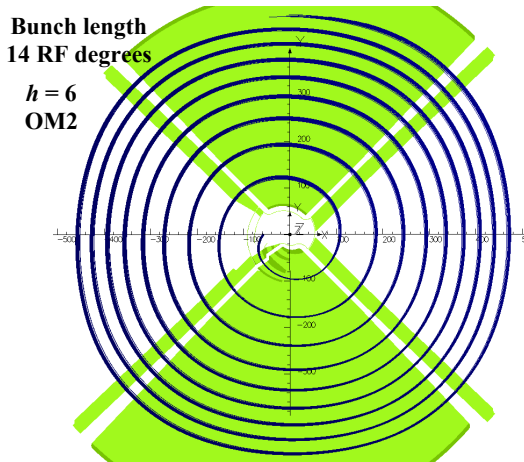

Figure 6: Using OM2, the new calculated beam orbits in SPC2 for initial horizontal and vertical beam emittance of 10 π mm.mrad and a longitudinal bunch length of 14 RF degrees, are shown superimposed on the lower half of the model of the acceleration electrodes.
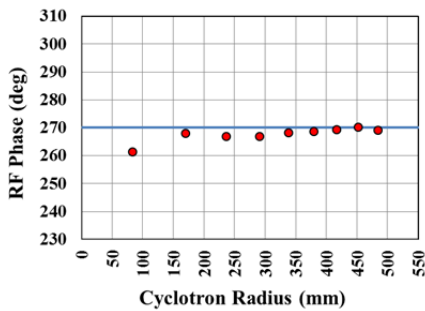

Figure 7: The calculated phase history of the central particle with its 9 crossings of the first acceleration gap, calculated with the better optimized beam (OM2) at harmonic number 6. The solid horizontal line at 270° represents the peak of the RF phase at gap 1.

Analysis of the beam transmission through the inflector showed large defocussing of the beam, especially in the vertical direction. This was later confirmed by visual inspection of the surfaces around the 10 mm high entrance window of the puller channel. Thus, with larger beam emittance beam losses can be expected at the puller window, which is located about 60 mm downstream from the inflector. Back-tracking of phase ellipses through the inflector to the injection line showed unattainable injection conditions, as is graphically illustrated in Fig. 8 with tracked orbits through the inflector.
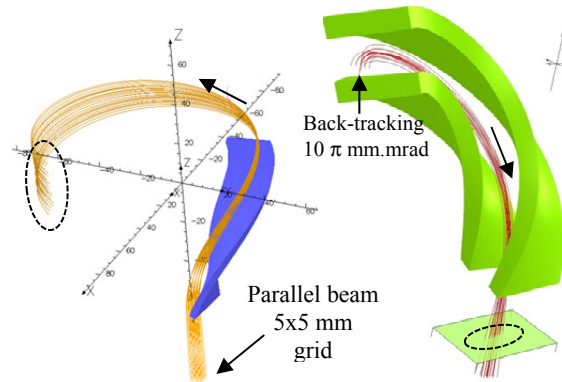

Figure 8: The strong beam defocussing effect of the inflector is illustrated in the left hand picture by the forward tracking of 25 particles, all starting parallel to the vertical injection axis (Z) from a 5x5 mm grid. One electrode plate was removed in the illustration. On the right hand side is the back-tracking calculation of a beam of particles with a horizontal and vertical phase-ellipse of 10 π mm.mrad.

The strong vertical defocussing in the inflector is quantified with the calculated transmission results, as shown in Fig. 9 for the back-tracking of horizontal and vertical emittance of 10 π mm.mrad. The vertical divergences will, with the high intensity beams, result in beam losses at the puller window.
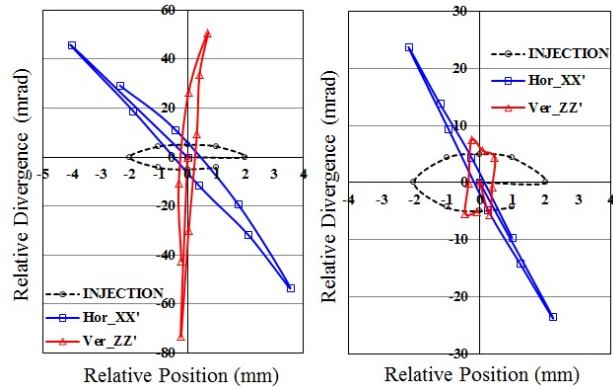

Figure 9: The calculated transmission through the inflector with an injected emittance of 10 π mm.mrad (dashed line) is shown, respectively, for the horizontal (figure on the left) and vertical (figure on the right) phase spaces. The cross-coupling to the horizontal (XX') and vertical (ZZ') phase spaces for both of the injected phase ellipses is evident.

Acceleration of $^{20}Ne^{3+}$ to 3.81 MeV at a harmonic number of 2 was also studied, even though the required frequency of 4 MHz is beyond the range of the RF system of SPC2. A horizontal and vertical emittance of 10 π mm.mrad was again tracked for each of three reference particles. The transit-time factors are 0.992 and 0.985 for the puller gap and subsequent 3 gaps, respectively.

For the two harmonic numbers, 6 and 2, and two optimization methods, OM1 and OM2, beam bunches of 14 RF degrees were compared after one turn in the cyclotron, at the EEC and at extraction. OM2 significantly improved the beam quality and consequently will improve the transmission efficiency. The calculated beam characteristics are listed in Table 1.

Table 1: Beam Quality Comparison

Harmonic number	6	6	2	2
Optimization Method	OM1	OM2	OM1	OM2
Radio-frequency (MHz)	12.16	12.16	4.053	4.053
Acceleration voltage (kV)	43.9	41.5	38.1	38.1
Bunch length (RF degrees)	14	14	14	14
Energy after 1 turn (MeV)	0.417	0.401	0.478	0.478
Energy spread after 1 turn	30.7%	6%	4.8%	1.3%
Extraction energy (MeV)	4.02	4.04	3.97	4
Extraction energy spread	3%	1.5%	2.2%	0.9%
Radial width at EEC (mm) [energy spread+emittance]	11	9	9	5
Radial width at EEC (mm) [energy spread]	7.2	3.6	5.3	2.2

The kinetic energies after one turn in the cyclotron were calculated in a vertical plane on a radial line along the centre of a valley and are shown in Fig. 10.
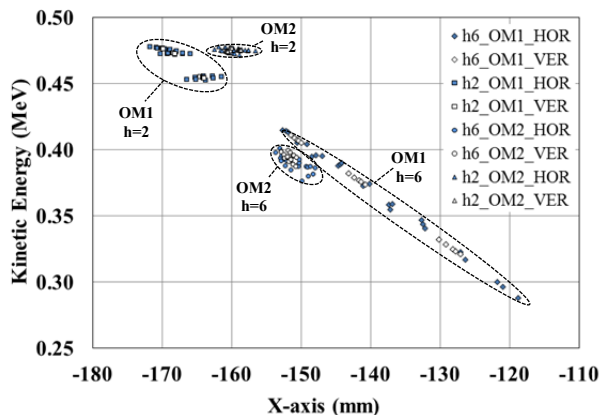

Figure 10: The beam bunch energies after 1 turn, obtained at harmonic numbers 6 and 2, for the two optimization methods.

For OM1 and harmonic number 2 a bunch length of 28 RF degrees was extracted with an energy spread of 4.2% at 4 MeV. The corresponding radial beam width due to the energy spread and emittance is 13 mm.

Using OM2 with 28 RF degree beam bunches for harmonic numbers 6 and 2, energy spreads of 4.8% and 3.2% were respectively obtained at extraction energy 4 MeV. The radial beam widths due to the energy spread and emittance are 16 mm and 10 mm, respectively.

CONCLUSIONS AND REMARKS

This study of the beam transmission through SPC2 led to the construction of several simulation models. The associated beam analysis methods and tools for 3D particle tracking can be used with any cyclotron.

The method used for minimizing the energy spread at extraction only, cannot fully compensate for the energy spread induced at the first few acceleration gaps. Large beam losses are to be expected in SPC2 with this method at harmonic number 6.

The transmission can be improved by more stringent beam optimization methods. It involves field and phase optimization, starting from the first turn in the cyclotron. The optimization methods will be studied further and implemented together with more diagnostic equipment, including a phase probe on a radial line in the cyclotron.

The spiral inflector also contributes to poor transmission through SPC2, due to its large vertical defocussing effect on the beam. An improved inflector design with significant improvement in the beam characteristics has been made.

The calculated databases will be implemented with OPAL-CYCL to calculate space-charge effects with high-intensity beams in SPC2.

The new user-friendly method of predicting isochronous magnetic fields for SPC2 from a calculated set of databases is a valuable improvement to cyclotron operation at iThemba LABS.

ACKNOWLEDGEMENTS

REFERENCES

[1] Z. B. du Toit *et al*., "Commissioning of the injector cyclotron for polarised and heavy ions at NAC", in *Proc. 14th Int. Conf. on Cyclotrons and their Applications*, Cape Town, South Africa, 1995, pp. 28-31.

[2] OPERA-3d, http://operafea.com

[3] A. Adelmann, C. Kraus, Y. Ineichen, S. Russel, and J. J. Yang, "The OPAL framework - User's reference manual", PSI Technical Report No. PSI-PR-08-02, 2008.

[4] J. J. Yang, A. Adelmann, M. Humbel, M. Seidel, and T. J. Zhang, "Beam dynamics in high intensity cyclotrons including neighbouring bunch effects: model, implementation and application", *Phys. Rev. ST Accel. Beams*, 064201, 2010.

[5] List of cyclotrons and booster-rings, in *Proc. 14th Int. Conf. on Cyclotrons and their Applications*, Cape Town, South Africa, 1995, entry C52, p747.

[6] J. L. Conradie *et al*., "Status report and new developments at iThemba LABS", in *Proc. 20th Int. Conf. on Cyclotrons and their Applications*, Vancouver, Canada, 2013, MOPPT032, p95.

[7] *OPERA-3d Reference Manual*, Ver. 17R1, pp 887-888.